Journal of Applied Polymer Science

Manufacturing and mechanical characterization of perforated hybrid composites based on flexible polyurethane foam

Ching-Wen Lou,[1] Shih-Yu Huang,[2] Ruosi Yan,[3] Jia-Horng Lin[2,4,5]

[1]Institute of Biomedical Engineering and Materials Science, Central Taiwan University of Science and Technology, Taichung 40601, Taiwan

[2]Laboratory of Fiber Application and Manufacturing, Department of Fiber and Composite Materials, Feng Chia University, Taichung City 40724, Taiwan

[3]School of Textiles, Tianjin Polytechnic University, Tianjin 300387, China

[4]School of Chinese Medicine, China Medical University, Taichung 40402, Taiwan

[5]Department of Fashion Design, Asia University, Taichung 41354, Taiwan

Correspondence to: J.-H. Lin (E-mail: jhlin@fcu.edu.tw)

ABSTRACT: This study focused on the fabrication and mechanical evaluation of nonwoven reinforced flexible polyurethane foam composites. Effects of perforation ratio, aperture size, and perforation depth on bursting and low-velocity impact responses of perforated composite panels were investigated. The nonwoven fabric used for cover sheet was composed of flame retardant polyester, low-melting point polyester, and recycled Kevlar staple fibers. Blending ratio of Kevlar fiber was confirmed to have relation to mechanical mechanism of cushioning layer. The highest mechanical strength value was obtained at 5 wt % of Kevlar ratio because of the highest cohesive force among recycled Kevlar, flame retardant polyester, and low-melting point polyester fibers was provided at the blending ratio. The perforated high-density flexible polyurethane foam composites panel was adhered with intra-ply hybrid laminates with various areal densities on each face to form sandwich structural composites. The results revealed that perforation ratio and aperture significantly influenced the bursting and low-velocity impact resistance behaviors of the perforated composites panel. Perforated composites with 10% perforation ratio and 4 mm aperture lead to maximum bursting strength of 437 N. Additional hybrid laminates significantly promoted the maximum bursting strength of the semiperforated hybrid composites by 212%. © 2015 Wiley Periodicals, Inc. J. Appl. Polym. Sci. **2015**, *132*, 42288.

KEYWORDS: fibers; foams; manufacturing; mechanical properties

Received 16 October 2014; accepted 31 March 2015

DOI: 10.1002/app.42288

INTRODUCTION

Foam-based sandwich composites have been extensively used in aerospace, automobile, and architectural industry for their excellent properties like light weight, ease of machining, and multistructure, or hybrid structure. Sandwich structural composites based on honeycomb, metal foam, and polymer foam core are widely used.[1–6] To increase functionality, metal plate and fabric are commonly used as face sheet of the sandwich composites.[7,8] Reinforcing face sheet and core structure, which are utilized to reinforce the integrity and enhance the load buffering capacity, respectively.

Previous researches focused on the influences of composite structure, such as face sheet composition, foam density, foam structure, and reinforcing beam, on the mechanical properties of the foam composites. In construction application, perforated structure panel are usually made of wood, metal, polymer, and rigid foam which performed excellent in sound absorption properties.[9–12] Porous materials, including fiber assembles and foam, also have high absorption coefficient at mid-high frequencies, which is higher than 500 Hz, because acoustic energy transfer to thermal energy.[13] As perforated panels made of rigid materials like wood and polymer have single acoustic principle and are crackable, which reduce service life, composite structure prefer to achieve aim of enhancing strength and acoustic absorbing capacity. Therefore, composite structure is essential to improve strength of acoustic absorbent materials.

Kevlar fiber performs high tenacity and high cut resistance and is widely used for military and civil applications. Many researches focused on Kevlar reinforced composites to investigate the enhancement of mechanical properties.[14–16] It can be seen that material strength is enhanced by high tenacity Kevlar

in the form of both fabric and loose fiber and the corresponding composites take advantages of light weight and ease of manufacturing.

Thermal-bonding is a process to heat fiber materials and cause partly melting, generating web structure among fibers.[17] The web structure can improve the tensile modulus, bending rigidity, and shear modulus of nonwoven fabrics.[18,19] Thermal bonding is commonly realized by infrared bonding, ultrasonic bonding, heated roller pressing, etc.[17]

The advantages of nonwoven fabric include easy manufacturing, fast production speed, and product variety. Staple fiber and filaments are both applied for nonwoven fabrics which are widely used in industrial application.[20–22] Flexible foam is usually made of polyols and isocyanate through foaming, which generated a quantity of carbon dioxide, and cross-linking reaction, which generate the unique cross-linked network inner structure.[23] Datta *et al.* investigated the thermal properties and dynamic mechanical performance of the synthetic flexible foam with various blending ratios.[24–27] The foam structure offers the flexible foam with elastic and resilient properties which is considered to enhance the energy storage capacity of the materials. Therefore, the flexible foam materials are widely used in cushioning application, such as filler of mattress and auto interior decoration.

In this study, intra-ply hybrid nonwovens laminated flexible polyurethane foam-based composites are fabricated. The center layer was composed of high-density flexible foam panel with various perforation forms. The intra-ply hybrid laminates help to improve the integrity of the sandwich structure to enhance the tensile resistance and the load buffering capacity of the center ply. Rigid materials were commonly used for impact energy absorption in the previous researches. However, the relative investigations on flexilbe foam materials are very rare and even none for the perforated structure. Therefore, the flexible foam-based composites in the present study provides an innovated composites mode. Intra-ply hybrid nonwoven which is composed of flame retardant polyester, low-melting point polyester, and recycled Kevlar staple fiber is laminated as the face sheet. Excellent mechanical properties and flame retardance are cohered to meet the industrial requirements. Mechanical properties and energy absorption of the intra-ply hybrid nonwoven fabric and the perforated hybrid composite were studied. Effects of perforation varieties on the impact behavior of the perforated hybrid composites were investigated. The mechanisms of energy absorption and dissipation were discussed. Additional intra-ply hybrid laminates were adhered to each surface of the perforated composite panels with various stacking sequences to determine their improvement of energy absorption.

EXPERIMENTAL

Materials

Biocomponent sheath-core polyester staple fiber (LPET, Far Eastern New Century Corporation, Taiwan) had a fineness of 4 Denier (D) with a length of 51 mm. LPET was composed of low-melting point polyester sheath which melts at 110°C, and common polyester core with melting point at 265°C. 6D Flame retardant polyester (FRPET, Far Eastern New Century Corporation, Taiwan) with a length of 51 mm had limit oxygen index (LOI) of 37. Recycled Kevlar staple fibers were uni-dimensional selvages supplied from Formosa Taffeta, Taiwan. High-density flexible polyurethane foam was synthetized from two-component APEXLON® reagents: polyols and isocyanate (Kuang Lung Shing Corporation, Taiwan). Biocomponent adhesive, which was utilized to laminate the additional hybrid laminates on the perforated composites, was supplied from Art Giant Technology Corporation.

Fabrication of Perforated Sandwich Composites

The perforated composite panel consisted of double intra-ply hybrid nonwoven face sheets and a transversal high-density flexible foam interlayer. Intra-ply hybrid nonwoven face sheet was manufactured via carding, laying, and needle-punching. According to function, the face sheet has two classifications: flame retardant layer, which is composed of FRPET and LPET in weight ratio of 90 : 10 with LOI of 30; and cushioning layer, which is composed of FRPET/Kevlar/LPET fibers with various blending ratios of 90 : 0 : 10, 85 : 5 : 10, 80 : 10 : 10, 75 : 15 : 10 and 70 : 20 : 10. Then, the nonwoven fabric was hot pressed by heated rollers at 0.5 rpm/min of 120°C. Tensile, tearing, bursting, and low-velocity impact properties of the nonwoven fabrics were studied. The sample with optimum mechanical performance was selected to produce the final intra-ply hybrid cushioning laminates by stacking, needle-punching and hot pressing.

Perforated composites panel was manufactured by perforating the flexible foam-based hybrid composites with various specifications. To begin with, reagents of polyols and isocyanate were mixed at stirring speed of 1200 rpm with a ratio of 8 : 2 in weight. The hardener which was purchased from KLS Corporation, Taiwan, was a mixture of toluene diisocyanate and polymeric methylene diphenyl diisocyanate at a weight ratio of 8 : 2. The materials mixed uniformly for 15 s at 25°C under standard atmospheric pressure. Then, the mixture was infused in to a metal mold with a dimension of 350 × 330×20 mm and double layers of intra-ply hybrid nonwovens had been laid at the bottom and top of the mold after 60 s of mixture reaction. The mixture was very viscous which has a viscosity of 2200 CPS and the polymer stopped expanding and cured quickly after approximately 10 s. The expansion factor of the foam was maintained at 4 by the mold pressure and the density was consequently kept at 250 kg/m^3.

From the inner structure illustration of Figure 1, it can be found that the high-density flexible foam has open cell structure. The cell has circular shape and uniform size. The diameter of the cell was 154.17 ± 33.30 μm and the wall thickness was 53.99 ± 9.72 μm. The maximum tensile strength of the flexible foam was 25.76 ± 2.74 N and the tensile elongation $196.29 \pm 6.93\%$, which was measured according to ASTM D3574 TEST E.

The metal mold was sealed before the mixture keeping foaming and expanding under pressure. The panel was demold after curing for 2 hours at 25°C under constant temperature and humidity condition. The resulting composite panel was perforated with circular aperture through punching machine. Influencing

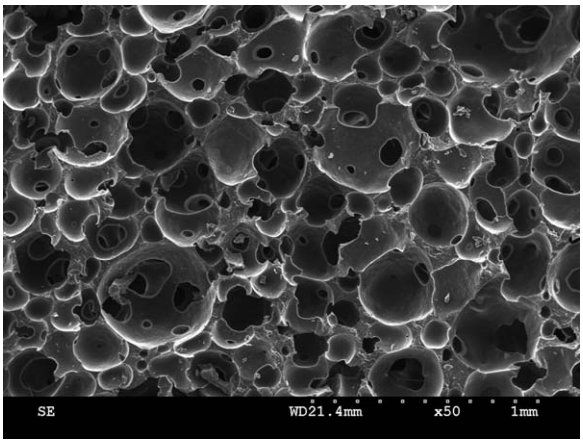

Figure 1. SEM photography of the high-density flexible foam.

factors, including aperture size, perforation ratio, and depth were applied to investigate their influences on the mechanical properties of the perforated hybrid composites. The aperture size of the perforated composites was controlled by the drill diameter of the mechanical drilling machine. The mathematical relationship among perforation ratio, aperture size, and distance is deduced as the following equation:

$$\text{Perforation ration} = \frac{R^2 \times 78.50}{K^2} \times 100 \quad (1)$$

where R is aperture size (mm) and K is distance between holes (mm). The perforation depth is defined as the ratio of the hole depth to the original thickness of the composites. The perforation depths of 25%, 50%, 75%, and 100% indicates the hole with 5, 10, 15, and 20 mm depths, respectively. The hole was manufactured with various perforation depths which was measured by vernier caliper and perforated by the automatic mechanical drilling machine to the calculated depth dimensions.

Figure 2 illustrates the structure of perforated composites and the parameter including aperture, distance, depth dimensions, and front and back faces. Specification of the perforated hybrid composites samples are presented in Table I. Effects of aperture size (AS) of samples ranging from 3 to 6 mm, perforation ratio (PR) varying from 5% to 20% with 5% intervals and perforation depth (PD) (semiperforated hybrid composites with 25%, 50%, and 75% perforation depths) on the mechanical properties of perforated hybrid composites were investigated. Semiperforated samples were loaded on the perforated face (F) and the corresponding back face (B), respectively. Responses of all the samples were evaluated under quasi-static and dynamic loading.

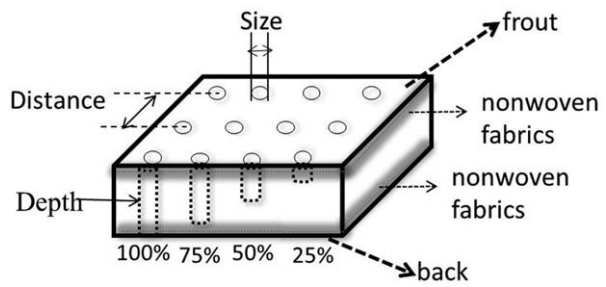

Figure 2. Schematic diagram of perforated hybrid composites.

Table I. Specifications of Perforated Composites Samples

Sample code	Aperture size (mm)	Perforation ratio (%)	Perforation depth (%)
AS-3	3	10	100
AS-4	4	10	100
AS-5	5	10	100
AS-6	6	10	100
PR-5	4	5	100
PR-10	4	10	100
PR-15	4	15	100
PR-20	4	20	100
PD(F)-25	4	10	25
PD(F)-50	4	10	50
PD(F)-75	4	10	75
PD(B)-25	4	10	25
PD(B)-50	4	10	50
PD(B)-75	4	10	75

Additionally, the intra-ply hybrid laminates with various areal densities adhered on tops and bottoms of the perforated panels to form sandwich hybrid composites to test their improvement on the mechanical properties. The hybrid laminates and flexible foam-based perforated composites where laminated together by biocomponent adhesive. The fixed amount of adhesive was coated on the hybrid nonwoven fabric homogenously by the coating machine, which could adjust the distance between scraper and the materials for 1 mm. Double layer of laminates with different areal densities stuck on the perforated panel, which were positioned free of pressure at 25°C for 24 hours for drying. As shown in Table II, four layer laminates (totally 1000 g/m^2) were distributed on front and back faces to investigate the effect of stacking sequence on the mechanical properties of composites.

Testing

Tensile Testing. Tensile testing of intra-ply hybrid nonwovens was conducted by Instron 5566 according to ASTM D5035. Specimens were trimmed to 25.4 mm × 180 mm rectangles on

Table II. Specifications of Sandwich Hybrid Perforated Panels

Sample code	Aperture size (mm)	Perforation ratio (%)	Perforation depth (%)	Hybrid laminates layer[a] (front/back)
HL0/4	4	10	50	0/4
HL1/3	4	10	50	1/3
HL2/2	4	10	50	2/2
HL3/1	4	10	50	3/1
HL4/0	4	10	50	4/0

[a] Areal density of single layer was 250 g/m^2.

Table III. Mechanical Properties of Intra-Ply Hybrid Nonwovens

FRPET/Kevlar/LPET blending ratio (%)	Tensile strength (N)		Tearing strength (N)		Bursting strength (N)	Residual force (N)
	CD	MD	CD	MD		
90 : 0 : 10	138 ± 9.45	64 ± 4.07	222 ± 12.35	131 ± 18.53	159 ± 11.45	8963 ± 103.36
85 : 05 : 10	195 ± 8.61	74 ± 2.44	303 ± 23.53	157 ± 5.01	240 ± 11.44	8633 ± 51.88
80 : 10 : 10	169 ± 8.82	70 ± 3.51	250 ± 17.27	148 ± 13.45	284 ± 22.71	8673 ± 248.67
75 : 15 : 10	195 ± 22.72	69 ± 7.28	297 ± 17.85	136 ± 19.2	213 ± 26.43	8729 ± 359.51
70 : 20 : 10	252 ± 9.68	93 ± 8.91	345 ± 26.75	185 ± 29.5	292 ± 35.45	8643 ± 201.07

both cross machine direction (CD) and machine direction (MD). The distance between a pair of pneumatic clamps was initially set at 75 mm. The cross head tensile speed was 300 ± 10 mm/min. Ten specimens were tested for each sample.

Tearing Testing. Tearing testing of intra-ply hybrid nonwovens was carried out through trapezoid procedure by ASTM D5587. A specimen with a dimension of 75 × 150 mm had a 15 mm-long preliminary cut at the center of the 75-mm edge. Set the distance between the clamps at 25 mm and the testing speed to 300 ±10 mm according to ASTM D5587. Ten specimens were tested on both CD and MD.

Bursting Strength Testing. Bursting strength test was conducted by Instron 5566 based on ASTM D3787. The specimen (150 mm × 150 mm) was fixed on the fixture and was loaded by a 25.4 ± 0.005 mm- diameter hemispherical-end foot at 100 ± 10 mm/min cross-head speed. The maximum load was recorded as the bursting strength of the specimen. Ten specimens were measured in each group.

Low-Velocity Impact Testing. Low-velocity impact test employed a drop-tower system (Kuang Neng Factory, Taiwan). The 9.4 kg drop-weight tup fell freely from approximately 65 mm to ensure incident force remain 9.0 kN. A 100 × 100 mm^2 specimen was placed on the bottom platform with a load cell at the center. Five specimens were measured in each group.

SEM Characterization. Scanning electron microscopy (SEM) images were acquired with a Hitachi S-3000N, Japan. A specimen was fixed in the SEM after precise treatment, including trimming, vacuum drying, and metallizing.

RESULTS AND DISCUSSION

Mechanical Properties of Intra-Ply Hybrid Nonwovens

Effects of recycled Kevlar blending ratio on the mechanical properties of intra-ply hybrid nonwovens are shown in Table III. The samples containing 5 and 20 wt % Kevlar staple fiber exhibited the optimum overall performance. 5 wt % Kevlar fiber reinforced the tensile and tearing resistance of hybrid nonwoven layer which were higher than nonreinforced nonwoven fabric. With the increase of Kevlar content to 10 and 15 wt %, the mechanical properties, however, tended to decrease. This is because that Kevlar fiber has smooth and low fictional surface, and cohesive force between Kevlar and FRPET and adhesion force between Kevlar and LPET are both decreased with the increase of Kevlar content. Kevlar fiber presents much higher modulus than because aromatic group takes place of aliphatic group in molecule segment. Thus, when it was promoted to 20 wt %, Kevlar fiber played dominant role in the reinforcement through thermal bonding so that the hybrid nonwovens performed highest resistance to tensile and tearing. Quasi-static bursting and low-velocity impact behavior exhibited similar variation tendencies with increasing Kevlar content. As hybrid nonwoven samples with 5 wt % and 20 wt % Kevlar performed similar mechanical properties, and to consider better cohesive force and to be economical, FRPET/Kevlar/LPET with blending ratio of 85 : 5 : 10 was selected to be the reinforcing face sheet of the perforated composites panel.

Effect of Aperture Size

In the present study, double hybrid nonwoven layers were laminated on both faces of the high-density flexible polyurethane foam before being perforated according to the various experimental designs to reinforce the fragile foam structure and keep integrity during repeated use.

Figure 3 illustrates the quasi-static bursting and low-velocity impact behaviors of perforated composites panels with 10% perforation ratio as increase of aperture size. Quasi-static bursting test was conducted by a hemispherical-end foot loading the sample with a constant rate. The whole vertical structure was compressed by the loading foot while the whole parallel structure was stretched and deformed because the face sheet restricted the whole structure to dissipate loading energy to wider area (Figure 4). As can be seen from Figure 3(a), bursting strength of AS-3, AS-4, AS-5, and AS-6 with hole sizes of 3, 4, 5, and 6 mm exhibits 27%, 14%, 6%, and 5% lower than non-perforated composites. On the base of 10% perforation ratio, K^2 is proportional to R^2 according to eq. (1). Therefore, AS-3, which had the lowest aperture size and the lowest distance between holes, gained the lowest supporting so that the bursting strength was the lowest. With the aperture size increasing from 4 to 6 mm, wider solid area ruptured and the bursting strength of the perforated composites was enhanced.

Low-velocity impact resistance was to evaluate the dynamic cushioning capacity of the perforated composites. High dynamic cushioning capacity results low residual force. Figure 3(b) shows that AS-3 and AS-4 had a slighter difference with no-perforated composites than AS-5 and AS-6. Contact area between the tup and sample surface decreased with the increasing of aperture size with in the supporting area. Thus, cushioning capacity decreased with the increase of contact area to absorb incident

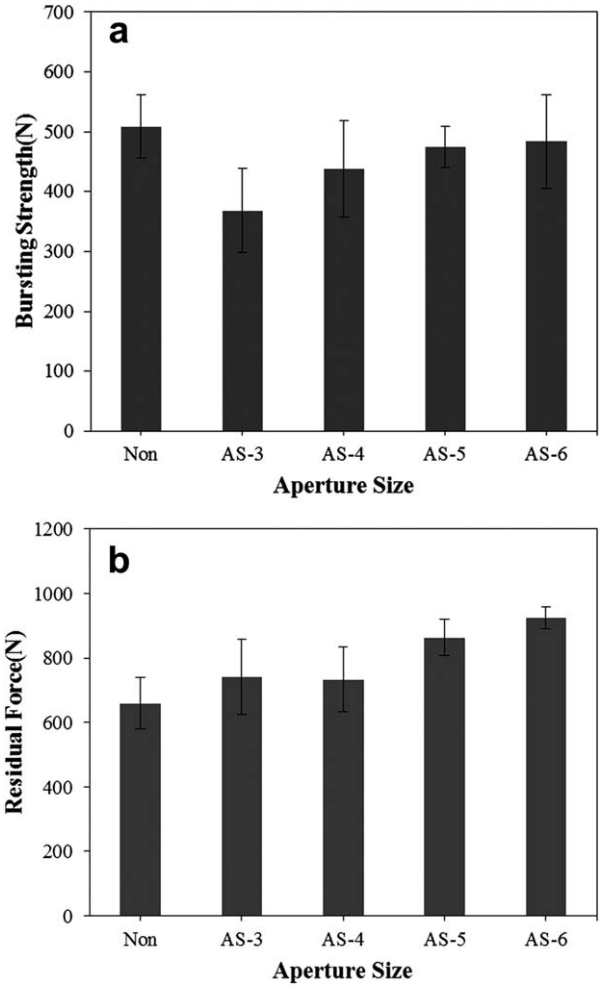

Figure 3. Quasi-static bursting (a) and low-velocity impact (b) behavior of nonperforated composites and hybrid composites panels as increase of aperture size (3, 4, 5, and 6 mm).

energy. AS-4 performed the lowest residual force which might because sample with 10% perforation dissipated energy effectively at 4 mm-size. For AS-5 and AS-6, samples, the aperture sizes were too large (5 and 6 mm, respectively) and the instantaneous dissipation capacity deceased.

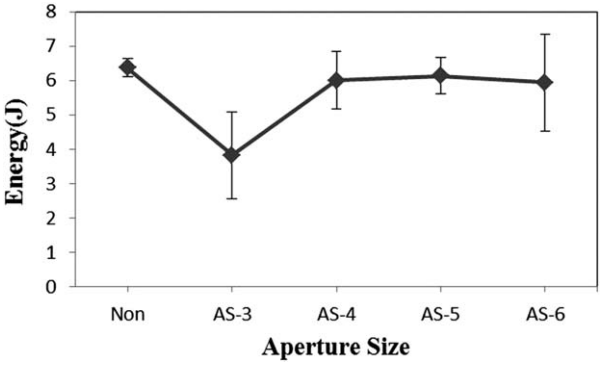

Figure 4. Effect of aperture size on fracture energy of hybrid composites panels.

Figure 4 presents the effect of aperture size on fracture energy of perforated hybrid composites panel. As shown in the figure, facture energy of nonperforated composites was 6.38 J while the value of all the perforated composites AS-3, AS-4, AS-5, and AS-6 were lower which are 3.83, 6.01, 6.14, and 5.94 J. The reason for AS-3 performing the lowest fracture energy was that according to eq. (1), the distance between the two holes was the lowest and the minimum volume foam which connected holes was ruptured by the lowest energy.

Effect of Perforation Ratio

Figure 5 depicts the effects of perforation ratio on the quasi-static bursting and low-velocity impact response of perforated hybrid composites with constant aperture size of 4 mm. It is worth noting that the static and dynamic properties exhibit similar tendencies. The higher the perforation ratio was, the closer the distance between neighboring holes was. The failure mechanisms of bursting were mainly, to begin with, the composites sustained the static loading by cell collapse which exhibited high load; then, the deformed and collapsed cell structure perform decreased strength; finally, rupture of the cell wall. As shown in Figure 5(a), the bursting strength decreased with increasing perforation ratio because of the decreased area rupturing. In terms of low-velocity test, the main mechanism of

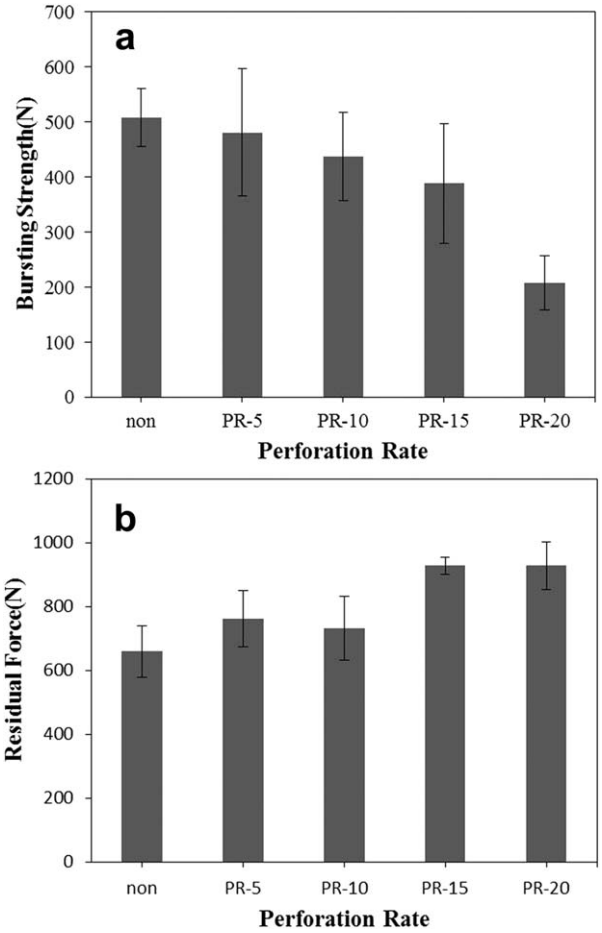

Figure 5. Effects of perforation ratio on the (a) bursting strength and (b) low-velocity impact resistance of hybrid composites.

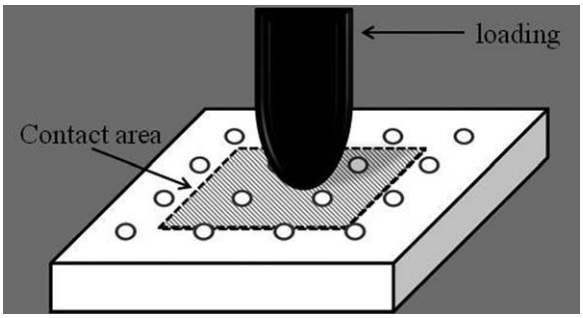

Figure 6. Schematic of bursting test of perforated hybrid composites.

energy absorption and dissipation was cell collapse. If the incident energy cannot be totally absorbed by the composites, the impactor would rebound and the unabsorbed energy turned to be gravitational potential energy. Figure 5(b) shows that residual force of PR-5 and PR-10 were higher than nonperforated composites, which performed the lowest residual force, for just 1% and 0.88%. Nonperforated sample had intact structure and totally contacted the drop weight impactor to convert the incident energy to compression potential energy. Cushioning force of PR-10 performed a slightly higher than PR-5 because the contact foam area was larger and the specific perforation structure could dissipate energy effectively (as shown in Figure 6). Figure 7 depicts the fracture energy of hybrid composites with various perforation ratios. The fracture energy values of PR-5 and PR-10 were higher which means that the bursting and impact resistance were superior in the structure.

Effect of Perforation Depth and Direction

Comparisons of static and dynamic loading behavior of perforated and nonperforated composite panels have been discussed. In this section, effects of perforation depth and direction on the semiperforated hybrid composite panel are studied in this section (Figure 8). As shown from Figure 8(a,b), the effect on quasi-static bursting behavior was more significant than that of low-velocity impact. Compressive capacity is the dominant factor of bursting resistance. Cell wall sustian the most loading by collapse and rupture. About 25% semiperforated composite panel provide the maximum volume of foam so that it can sustain highest load until rupture. About 50% semiperforated composite panel performed lower bursting strength than 25% panel on front side, but higher on back and the values on two faces

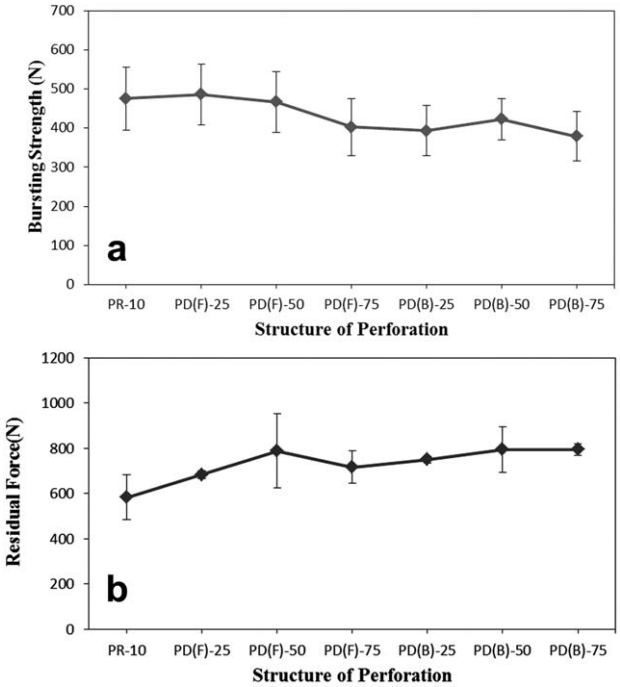

Figure 8. Quasi-static bursting (a) and low-velocity impact (b) behavior of semiperforated hybrid composites.

had minimum difference among the three samples, which meant that the factor of loading direction applied the minimal impact on 50% semiperforated composite. This is an advantage in inductrial application. About 75% semiperforated composite failed to support and dissipate energy, and exhibited the lowest bursting strength on both front and back face. Figure 9 illustrates fracture energy of semiperforated composites with different perforation depths. It is clear that the difference between PD(F)-50 and PD(B)-50 is the lowest among the samples which have same perforation depth but different loading face. The result demenstrates load buffering capacity on the two sides of 50% depth is the most balanced which has positive effect on load buffering ability of the perforated composites. As can be seen from the figure that fracture energy decreased linearly.

Effect of Intra-Ply Hybrid Laminates

According to the aforementioned results, hybrid nonwovens with FRPET/Kevlar/LPET blending ratio at 85 : 5 : 10 was

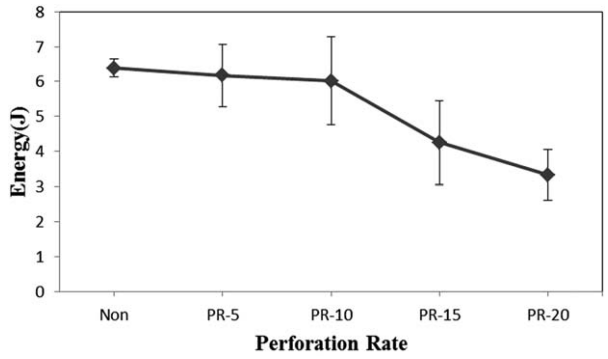

Figure 7. Effect of perforation ratio of hybrid composites on fracture energy.

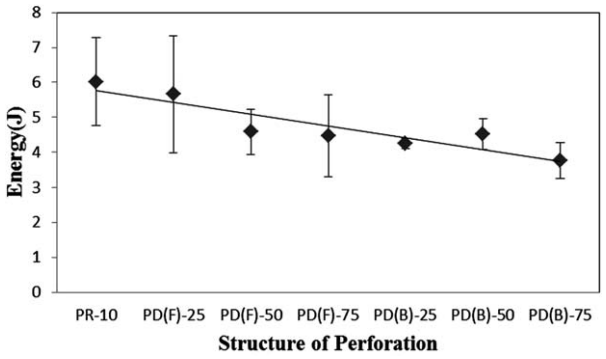

Figure 9. Fracture energy of semiperforated composites with different perforation depths.

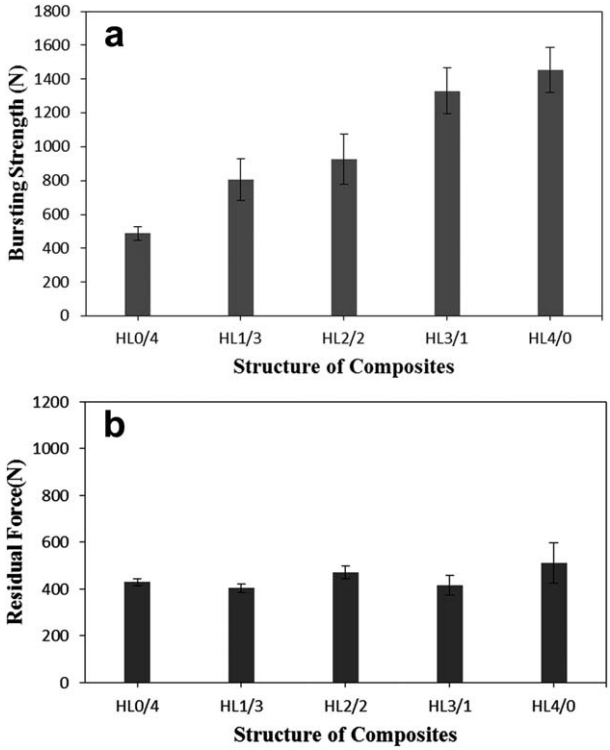

Figure 10. Effects of stacking sequence on (a) bursting strength and (b) low-velocity impact resistance of sandwich laminated perforated composites.

selected to fabricate the hybrid laminates. About 50% semiperforated hybrid composites with 4 mm aperture and 10% perforation ratio was selected to be the core material. The hybrid laminates and the flame-retardant layer was stacked and cohered by needle punching and thermal bonding and then laminated on both sides of the perforated composites panel by adhering. Quasi-static and low-velocity impact behaviors of the resulting hybrid composites were evaluated. As shown in Figure 10, bursting strength of the sandwich hybrid composites was enhanced with the increase of areal density of hybrid laminates on front face of 50% semiperforated hybrid composites. As the sample was loaded on the front face, the bursting resistance of additional

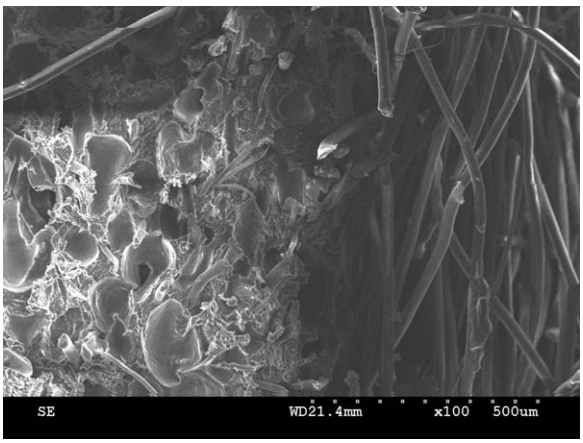

Figure 11. SEM photography of interlayer structure of sandwich laminated perforated composites.

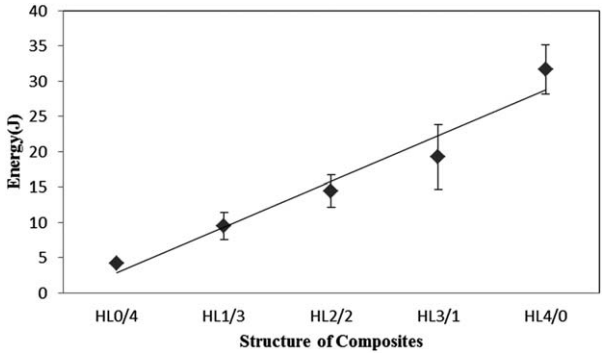

Figure 12. Fracture energy of sandwich laminated perforated composites with different stacking sequences.

laminates on the front face increased with the areal density increasing because more entangled and bonded fibers fractured and debonded. From Figure 10(a), it can be found that the failure of hybrid laminates on front face was a significant mechanism of bursting resistance. The thermal-bonded surface nonwoven laminates had high tensile and tear resistance. As high-density flexible foam has good adhesion with fibers based on its own stickiness (Figure 11), composites panel is loaded by the bursting end and spreads loading energy to wide deformation area. These mechanical properties increased with increasing areal density and thermal bonding points due to the cohesive force of enhancement and bonding force. From Figure 12, it can be seen that fracture energy of sandwich laminated semiperforated composites increases linearly with the increasing area density of front face and HL 4/0 provides the highest value. On the contrary, samples were shocked by drop-weight impactor and were loaded by instant impact. The composites were compressed in the whole thickness direction. As the total areal density of front and back faces are identical in every sandwich laminated perforated composite sample, the effect of laminates structure on load buffering capacity of the sample is not significant.

CONCLUSION

This study successfully prepared the nonwoven reinforced flexible polyurethane foam composites and evaluated mechanical properties. Results of FRPET/Kevlar/LPET hybrid nonwovens investigation revealed that Kevlar fibers had smooth surface and low cohesive force and 5 wt % Kevlar nonwovens with the optimum mechanical properties was selected.

Aperture size and perforation ratio both dominantly influenced the quasi-static bursting and low-velocity impact wave propagation. Perforated hybrid composites with 4 mm aperture size performed the highest ability to absorb and dissipate energy. Perforation depth play a less important role in bursting and impact behavior. Composites with perforation ratio at 10% provided the highest bursting strength and low-velocity impact resistance for optimum energy absorption. About 50% semiperforated hybrid composites panel had the lowest difference in two loading directions. Furthermore, the bursting strength of sandwich hybrid composites was promoted of approximatedly 66% when compared with perforated composites. The effect of

stacking sequence on the low-velocity impact resistance of sandwich hybrid composites was moderated.

REFERENCES

1. Xiong, J.; Zhang, M.; Stocchi, A.; Hu, H.; Ma, L.; Wu, L. Z.; Zhang, Z. *Compos. B Eng.* **2014**, *60*, 350.
2. Kang, K. W.; Kim, H. S.; Kim, M. S.; Kim, J. K. *Mater. Sci. Eng. A Struct.* **2008**, *483–484*, 333.
3. Li, S. Q.; Wang, Z. H.; Wu, G. Y.; Zhao, L. M.; Li, X. *Compos. A Appl. Sci.* **2014**, *56*, 262.
4. Sun, Z.; Hu, X. Z.; Sun, S. Y.; Chen, H. R. *Compos. Sci. Technol.* **2013**, *77*, 14.
5. Atas, C.; Sevim, C. *Compos. Struct.* **2010**, *93*, 40.
6. Nasirzadeh, R.; Saber, A. R. *Int. J. Impact Eng.* **2014**, *63*, 129.
7. Ma, P. B.; Zhang, F.; Gao, Z.; Jiang, G. M.; Zhu, Y. J. *Compos. B Eng.* **2014**, *56*, 847.
8. Ghalami-Choobar, M.; Sadighi, M. *Aerosp. Sci. Technol.* **2014**, *32*, 142.
9. Lin, M. D.; Tsai, K. T.; Su, B. S. *Appl. Acoust.* **2009**, *70*, 31.
10. Choy, Y. S.; Liu, Y.; Cheung, H. Y.; Xi, Q.; Lau, K. T. *J. Sound Vib.* **2012**, *331*, 2348.
11. Qian, Y. J.; Kong, D. Y.; Liu, Y.; Liu, S. M.; Li, Z. B.; Shao, D. S.; Sun, S. M. *Appl. Acoust.* **2014**, *82*, 23.
12. Jahani, D.; Ameli, A.; Jung, P. U.; Barzegari, M. R.; Park, C. B.; Naguib, H. *Mater. Des.* **2014**, *53*, 20.
13. del Rey, R.; Alba, J.; Arenas, J. P.; Sanchis, V. J. *Appl. Acoust.* **2012**, *73*, 604.
14. Yadav, S. N.; Kumar, V.; Verma, S. K. *Mater. Sci. Eng. B Solid* **2006**, *132*, 108.
15. Ramadhan, A. A.; Abu Talib, A. R.; Rafie, A. S. M.; Zahari, R. *Mater. Des.* **2013**, *43*, 307.
16. Nilakantan, G. *Compos. Struct.* **2013**, *104*, 1.
17. Michielsen, S.; Pourdeyhimi, B.; Desai, P. *J. Appl. Polym. Sci.* **2006**, *99*, 2489.
18. Wang, X. Y.; Gong, R. H.; Dong, Z.; Porat, I. *Wear* **2007**, *262*, 424.
19. Ramaswamy, S.; Clarke, L. I.; Gorga, R. E. *Polymer* **2011**, *52*, 3183.
20. Krucinska, I. *J. Electrostat.* **2002**, *56*, 143.
21. Acar, M.; Harper, J. F. *Comput. Struct.* **2000**, *76*, 105.
22. Hao, A. Y.; Zhao, H. F.; Chen, J. Y. *Compos. B Eng.* **2013**, *54*, 44.
23. Lee, S. T.; Ramesh, N. S. Polymeric Foams: Mechanisms and Materials; CRC Press: London, **2004**; Chapter 5&6, pp 139–174.
24. Datta, J. *J. Elastom. Plast.* **2010**, *42*, 117.
25. Datta, J.; Kacprzyk, M. *J. Therm. Anal. Calorim.* **2008**, *93*, 753.
26. Datta, J.; Rohn, M. *Polimery* **2008**, *53*, 871.
27. Datta, J.; Janicka, M. *Przem. Chem.* **2007**, *86*, 624.